



Article

PBMCs as Tool for Identification of Novel Immunotherapy Biomarkers in Lung Cancer

Caterina De Rosa ^{1,†}, Francesca Iommelli ^{2,†}, Viviana De Rosa ^{2,*}, Giuseppe Ercolano ³, Federica Sodano ³, Concetta Tuccillo ¹, Luisa Amato ¹, Virginia Tirino ^{4,5}, Annalisa Ariano ¹, Flora Cimmino ⁶, Gaetano di Guida ¹, Gennaro Filosa ¹, Alessandra di Liello ¹, Davide Ciardiello ⁷, Erika Martinelli ¹, Teresa Troiani ¹, Stefania Napolitano ¹, Giulia Martini ¹, Fortunato Ciardiello ¹, Federica Papaccio ⁸, Floriana Morgillo ^{1,‡} and Carminia Maria Della Corte ^{1,*}

- ¹ Department of Precision Medicine, University of Campania Luigi Vanvitelli, 80131 Naples, Italy; caterina.derosa1@unicampania.it (C.D.R.); concetta.tuccillo@unicampania.it (C.T.); luisa.amato@unicampania.it (L.A.); annalisaariano98@outlook.it (A.A.); gaetano.diguida@studenti.unicampania.it (G.d.G.); gennaro.filosa@unicampania.it (G.F.); alessandradiliello@gmail.com (A.d.L.); erika.martinelli@unicampania.it (E.M.); teresa.troiani@unicampania.it (T.T.); stefania.napolitano@unicampania.it (S.N.); giulia.martini@unicampania.it (G.M.); fortunato.ciardiello@unicampania.it (F.C.); floriana.morgillo@unicampania.it (F.M.)
- ² Institute of Biostructures and Bioimaging, National Research Council, 80145 Naples, Italy; francesca.iommelli@ibb.cnr.it
- ³ Department of Pharmacy, School of Medicine, University of Naples Federico II, 80138 Naples, Italy; giuseppe.ercolano@unina.it (G.E.); federica.sodano@unina.it (F.S.)
- ⁴ Department of Experimental Medicine, University of Campania Luigi Vanvitelli, 81100 Caserta, Italy; virginia.tirino@unicampania.it
- ⁵ U.P. Diagnostica Citometrica e Mutazionale, A.O.U. Vanvitelli, Università degli Studi della Campania, 80138 Naples, Italy
- ⁶ Hospital “Martiri Di Villa Malta”, 84087 Sarno, Italy; floracimmino81@gmail.com
- ⁷ Division of Gastrointestinal Medical Oncology and Neuroendocrine Tumors, European Institute of Oncology (IEO), IRCCS, 20141 Milan, Italy; davide.ciardiello@unicampania.it
- ⁸ Department of Medicine, Surgery and Dentistry, “Scuola Medica Salernitana”, University of Salerno, 84084 Baronissi, Italy; fpapaccio@unisa.it
- * Correspondence: viviana.derosa@ibb.cnr.it (V.D.R.); carminiamaria.dellacorte@unicampania.it (C.M.D.C.); Tel.: +39-0812203430 (V.D.R.); +39-3929160541 (C.M.D.C.)
- † These authors contributed equally to this work as co-first authors.
- ‡ These authors contributed equally to this work as co-last authors.



Citation: De Rosa, C.; Iommelli, F.; De Rosa, V.; Ercolano, G.; Sodano, F.; Tuccillo, C.; Amato, L.; Tirino, V.; Ariano, A.; Cimmino, F.; et al. PBMCs as Tool for Identification of Novel Immunotherapy Biomarkers in Lung Cancer. *Biomedicines* **2024**, *12*, 809. <https://doi.org/10.3390/biomedicines12040809>

Academic Editors: Umberto Malapelle and Luca Pacini

Received: 29 February 2024
Revised: 29 March 2024
Accepted: 3 April 2024
Published: 5 April 2024



Copyright: © 2024 by the authors. Licensee MDPI, Basel, Switzerland. This article is an open access article distributed under the terms and conditions of the Creative Commons Attribution (CC BY) license (<https://creativecommons.org/licenses/by/4.0/>).

Abstract: Background: Lung cancer (LC), including both non-small (NSCLC) and small (SCLC) subtypes, is currently treated with a combination of chemo- and immunotherapy. However, predictive biomarkers to identify high-risk patients are needed. Here, we explore the role of peripheral blood mononuclear cells (PBMCs) as a tool for novel biomarkers searching. Methods: We analyzed the expression of the cGAS-STING pathway, a key DNA sensor that activates during chemotherapy, in PBMCs from LC patients divided into best responders (BR), responders (R) and non-responders (NR). The PBMCs were whole exome sequenced (WES). Results: PBMCs from BR and R patients of LC cohorts showed the highest levels of STING ($p < 0.0001$) and CXCL10 ($p < 0.0001$). From WES, each subject had at least 1 germline/somatic alteration in a DDR gene and the presence of more DDR gene mutations correlated with clinical responses, suggesting novel biomarker implications. Thus, we tested the effect of the pharmacological DDR inhibitor (DDRi) in PBMCs and in three-dimensional spheroid co-culture of PBMCs and LC cell lines; we found that DDRi strongly increased cGAS-STING expression and tumor infiltration ability of immune cells in NR and R patients. Furthermore, we performed FACS analysis of PBMCs derived from LC patients from the BR, R and NR cohorts and we found that cytotoxic T cell subpopulations displayed the highest STING expression. Conclusions: cGAS-STING signaling activation in PBMCs may be a novel potential predictive biomarker for the response to immunotherapy and high levels are correlated with a better response to treatment along with an overall increased antitumor immune injury.

Keywords: PBMC; cGAS-STING; biomarker

1. Introduction

During the past years several new therapies have been developed for lung cancer (LC). Both non-small (NSCLC) and small lung cancer (SCLC) subtypes are currently treated with a combination of chemo- and immunotherapy, with variable duration of responses. In almost all patients, at variable time points disease progression occurs [1,2]. Thus, we still need novel biomarkers and novel potential combinations [3–5]. Nowadays, the overactivation of the PD-L1/PD-1 axis represents a good target and biomarker for cancer treatment, but it is not sufficient to identify immunotherapy-responsive patients and it is not able to reflect the dynamicity of immune response. In this respect, there is a need to use accurate predictive biomarkers for an early identification of responder (R) and non-responder (NR) patients. In this study, we hypothesized that certain biological parameters, which can be potentially detected in peripheral blood, could be used as surrogate biomarkers of a predictive tumor response [6,7]. Our group and others have demonstrated that activation of innate immune pathways in cancer cells, such as canonical cGAS/STING signaling [5], is a good predictor of antitumor immune response [3] and that exceptionally long R LC patients may harbor germline variants in DDR genes [8]. In the present work, we used peripheral blood immune cells (PBMCs) as a tool for investigating the innate immune response and as a source for genetic testing, proposing an innovative strategy for monitoring and predicting immunotherapy response.

2. Materials and Methods

2.1. Treatment and Study Assessments

We enrolled patients with a diagnosis of NSCLC or SCLC receiving one of the following treatments: chemotherapy (cisplatin) and/or an anti-PD-L1 antibody (atezolizumab, durvalumab). The patients were grouped as follows: best responders (BR) were considered as patients with controlled disease lasting more than 12 months in NSCLC and more than 6 months in SCLC, that were clinically relevant compared with registration clinical trials [9–11]; responders (R) were defined as patients achieving at least stable disease (SD) at first radiological assessment, while non-responders (NR) were defined as patients showing progression of disease (PD) as the best response.

2.2. Peripheral Blood Mononuclear Cells (PBMC) Isolation: Step-By-Step Method

Human samples were collected after obtaining a written informed consent from patients in accordance with the Declaration of Helsinki. The protocol for the use of these samples for research purposes was approved by the Ethics Committee of the University of Campania “Luigi Vanvitelli”, Naples (*n.* 280 on 16 May 2020). Lung cancer patients’ blood serum was collected by centrifugation and stored immediately at -20°C or prepared for the ELISA assay kit for the detection of CXCL10 and CCL5 (Invitrogen™, Santa Clara, CA, USA). Subsequently, peripheral blood was collected in BD vacutainer spray-coated K2EDTA tubes (BD, Franklin Lakes, NJ, USA) as described in our previous studies [8,12,13]. Within 2 h of blood draw, PBMCs were isolated by using Lymphosep (Aurogene Srl, Rome, Italy) gradient centrifugation. Furthermore, to eliminate the contamination of red blood cells (RBCs) in the PBMC samples, we suspended the PBMC pellets in the RBC lysis solution (Invitrogen™, Santa Clara, CA, USA). After several washes with PBS, PBMCs were transferred into TRIsure™ (Bioline, Meridian Bioscience, Memphis, TN, USA) and stored at -80°C until use or immediately resuspended in RPMI 10% FBS containing human autologous serum (10%), ultraglutamine I (1%), penicillin and streptomycin (1%). After isolation, immune cells were cultured in presence of beads coated with anti-CD3 and anti-CD28 (Life Technologies, Carlsbad, CA, USA) at a ratio of 1 bead per 10 cells and IL-2 (Miltenyi Biotech, Bergisch Gladbach, Germany) at a concentration of 20 U/mL. After 24 h

of culture, cisplatin 0.5 μM or DNA-PK-I 2 μM concentration was added for a further 72 h. Culture supernatants were collected for further analysis. Representative images shown in Figure 1 report a detailed scheme of the PBMC isolation method step-by-step.

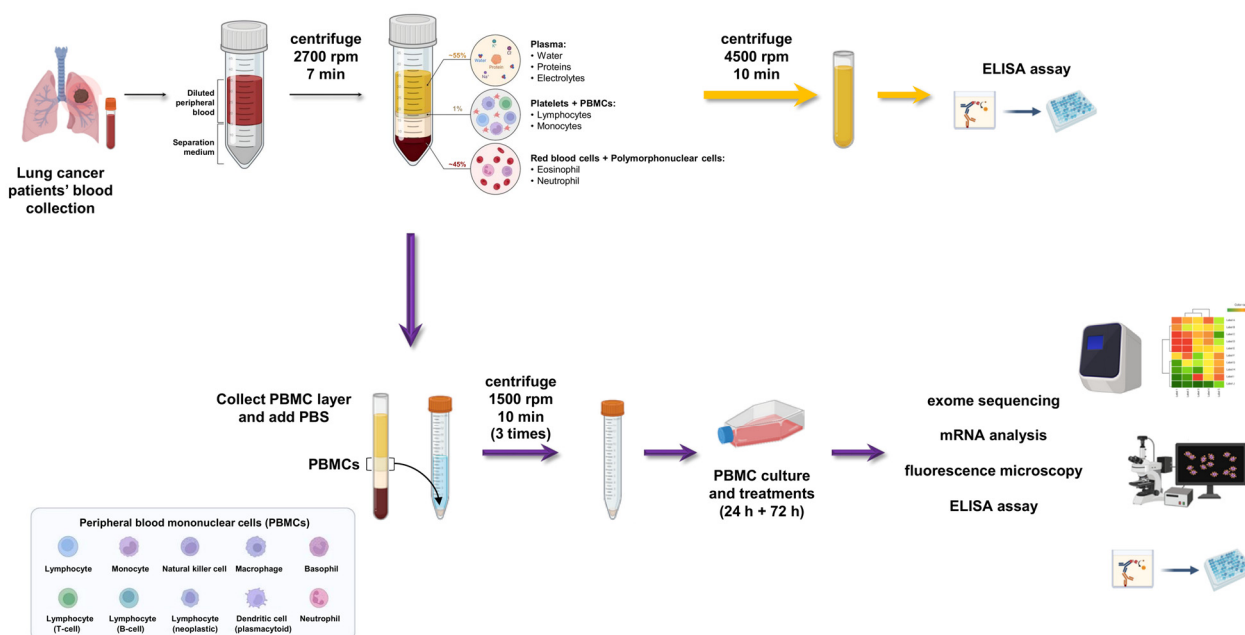


Figure 1. A graphical summary of the PBMC isolation method step-by-step. The graphical scheme was produced by the authors using the free BioRender platform.

2.3. Enzyme-Linked Immunosorbent Assay (ELISA)

The protein expression levels of extracellular cytokines and chemokines (CXCL10 and CCL5/RANTES) were measured in the blood serum of lung cancer patients, using the Human RANTES ELISA Kit (cat. No. EHRNTS) for CCL5/RANTES and Human IP-10 ELISA Kit (cat. No. KAC2361) for CXCL10 (Invitrogen; Thermo Fisher Scientific, Inc., Waltham, MA, USA). The amounts of proteins were measured in clear flat-bottom 96-well plates in accordance with the manufacturers' instructions. The optical density was determined using the Infinite M Plex (Tecan, Männedorf, Switzerland) microplate reader set to 450 and 550 nm. The readings at 550 nm were subtracted from the 450 nm reading to correct for optical imperfections in the plate. The concentrations (pg/mL) of the different proteins in each sample were determined by interpolating from the absorbance value (Y axis) to protein concentration (X axis) using the standard curve (Table S1). Each experiment was performed in duplicate. Data are expressed as mean \pm SD.

2.4. RNA Extraction and cDNA Synthesis

Total RNA was obtained from cell lines using TRIsure reagent (BIO-38033, Meridian Bioscience, Memphis, TN, USA), according to the manufacturer's protocol. Briefly, cells (5×10^6) were lysed with 1 mL of TRIsure and incubated for 5 min at RT. Chloroform (0.2 mL) was added and samples were shaken vigorously by hand for 15 sec and incubated for 3 min at RT. Samples were then centrifuged at $12,000 \times g$ for 15 min at 4 $^{\circ}\text{C}$. The samples separated into a pale green, organic phase, an interphase, and a colorless upper aqueous phase. The aqueous phase was removed for RNA extraction and transferred to another tube. RNA was precipitated by mixing with cold isopropyl alcohol (0.5 mL) for 2 h at -80 $^{\circ}\text{C}$. Samples were centrifuged at $12,000 \times g$ for 10 min at 4 $^{\circ}\text{C}$ and washed twice with 75% ethanol. Total RNA was suspended in 50 μL of RNase-free water. The purity and concentration of RNA were determined by OD 260/280 readings using the Nanodrop 2000 spectrophotometer (Thermo Fisher Scientific, Waltham, MA, USA). After RNA extraction, cDNA was generated from 500 ng of total RNA using a SensiFAST cDNA

Synthesis Kit (BIO-65053, Meridian Bioscience, Memphis, TN, USA) under the following conditions: 25 °C for 10 min, 42 °C for 15 min, 85 °C for 5 min.

2.5. Gene Expression Analysis by Quantitative qRT-PCR

mRNA expression levels of *STING*, *cGAS*, *CXCL10* and *CCL5* genes were evaluated by qRT-PCR with a QuantStudio 7-Flex (Applied Biosystems by Life Technologies, Monza, Italy) using the SensiFAST SYBR Hi-ROX Kit (BIO-92005, Meridian Bioscience, Memphis, TN, USA) under the following conditions: 50 °C for 2 min (stage 1) followed by a denaturation step at 95 °C for 10 min (stage 2) and then 40 cycles at 95 °C for 15 s and 60 °C for 1 min (stage 3). All samples were run in duplicate, in 20 µL reactions and relative expression of genes was determined by normalizing to *18S*, used as an internal control gene; to calculate relative gene expression in value we used the $2^{-\Delta Ct}$ or $2^{-\Delta\Delta Ct}$ method. Table 1 shows the list of primer sequences used for qRT-PCR.

Table 1. List of primer sequences used for qRT-PCR.

Gene	Forward Sequence	Reverse Sequence
<i>18S</i>	5'-CGCCGCTAGAGGTGAAATTC-3'	3'-CTTTCGCTCTGGTCCGTCTT-5'
<i>STING</i>	5'-CAGGCACTGAACATCCTCCT-3'	3'-ATATACAGCCGCTGGCTCAC-5'
<i>cGAS</i>	5'-CTCCACGAAGCCAAGACCTC-3'	3'-GCGGCTGAGCTTCAACTTCT-5'
<i>CCL5</i>	5'-CTCCCATATTCCTCGGACA-3'	3'-CTCTGGGTTGGCACACACTT-5'
<i>CXCL10</i>	5'-GGTGAGAAGAGATGTCTGAATCC-3'	3'-GTCCATCCTTGAAGCACTGCA-5'

2.6. Next-Generation Sequencing (NGS)

NGS analysis, alignment and filtering analysis were performed by the AMES service (Casalnuovo, Italy). Germline mutations were first filtered as a major allele frequency (MAF) of 0.01% in the database Exome Aggregation Consortium (ExAC-EAS). We then performed an analysis of germline variants which led to loss of function (LoF): (1) gain of stop codon, (2) loss of initiation codon, (3) frameshift, (4) deletion of single exon, (5) missense change and inframe del predicted by in silico tools as deleterious (poliphen-2 and SIFT) and reported in ClinVar database as pathogenic or uncertain significance variants.

2.7. Generation of 3D Spheroid Culture

NCI-H661 (ATCC CAT#HTB-183; RRID: CVCL_1577) and H460 (ATCC CAT#HTB-177; RRID: CVCL_0459) were maintained in RPMI 1640 (R8758, Sigma-Aldrich, Merck, Darmstadt, Germany) supplemented with 10% FBS (Sigma-Aldrich, Merck, Darmstadt, Germany) and 1× penicillin-streptomycin (P0781, Sigma-Aldrich, Merck, Darmstadt, Germany) in a humidity-controlled environment (37 °C, 5% CO₂). NCI-A549 (ATCC CAT#CCL-185; RRID: CVCL_0023) was maintained in DMEM (D5030, Sigma-Aldrich, Merck, Darmstadt, Germany) supplemented with 10% FBS and 1× penicillin-streptomycin in a humidity-controlled environment (37 °C, 5% CO₂). Cell lines were grown in standard culture conditions, harvested and dissociated into single cell suspensions for spheroid generation. Tumor spheroids were generated by seeding 10⁴ cells per well in ultra-low attachment (Corning, New York, NY, USA) round-bottom 6-well plates in the same culture media used for the monolayer cultures. Plates were incubated at 37 °C in 5% CO₂ and spheroids were maintained by performing medium replenishments every 3–4 days. Cancer cells started to form spheroids at day 1 and well-formed spheroids were seen at day 7.

2.8. Co-Localization of 3D Tumor Spheroids and LC Patient-Derived PBMCs by Immunofluorescence (IF)

Seven days after cell seeding, the spheroids were ready for co-culture. Co-cultures were started by adding 5 × 10⁵ LC patients-isolated PBMCs per well pre-treated with DNA-PK-I (2 µM) or cisplatin (0.5 µM) for 72 h. Before co-culture, 50 µM CellTracker Deep Red dye (Cat. No. C34565, Invitrogen, Carlsbad, CA, USA) was added to PBMC

culture medium for 45 min and 10 μ M CellTracker Blue CMAC (7-amino-4-chloromethyl coumarin) (Cat. No. C2110, Invitrogen, Carlsbad, CA, USA) was added to the spheroid culture medium for 45 min. After the staining, the PBMCs were added to spheroids and the co-cultures were performed for 72 h. After 72 h, the fluorescence was imaged using a Cell Discoverer 7 microscope (ZEISS Olympus, Nikon, Tokyo, Japan) at the facility center of CEINGE Biotecnologie Avanzate (Napoli, Italy). The quantification of the mean fluorescence intensity (MFI) was performed with ImageJ Software version 1.52e.

2.9. Flow Cytometry

After isolation, PBMCs from LC patients were stained and analyzed using standard flow cytometry approaches. Single cell suspensions from all samples were stained with Live Dead Blue (Invitrogen, Carlsbad, CA, USA, 1:400 in PBS) for 10 min at 4 °C, washed with FACS buffer (1% FBS in PBS) and then stained with cell surface marker antibodies for 45 min at 4 °C. For STING and Granzyme B staining, cells were fixed and permeabilized with FIX & PERM™ Cell Permeabilization Kit (Thermo Fisher Scientific, Waltham, MA, USA).

Antibodies used were anti-human CD3 (UCHT1, SK7), CD4 (L3T4, SK3), CD8 (SK1), CD14 (M ϕ P9), CD56 (NCAM16.2), CD19 (SJ25C1), CD16 (3G8) from BD Bioscience; anti-human STING (#90947) from Cell Signaling Technology, Danvers, MA, USA; and anti-human Granzyme B (REA226) from Miltenyi Biotech (Bergisch Gladbach, Germany). For STING labeling, a secondary FITC-labeled rabbit monoclonal antibody (Abcam, Cambridge, UK) was added at 4 °C for 30 min in the dark.

Labeled cells were washed and resuspended in FACS buffer for flow cytometric analysis on a BD Fortessa with FACS Diva software (BD Biosciences, Franklin Lakes, NJ, USA) and analyzed using FACS Diva software, version 8.0. Negative gating was based on a fluorescence-minus-one (FMO) strategy.

2.10. Multiplex Cytokine Assay

The concentrations of various cytokines in cell-free culture supernatants were determined using custom human LEGENDplex™ analyte assay kits (Biolegend Inc., San Diego, CA, USA). The assay was performed according to the manufacturer's instructions. Samples were acquired on a Bricyte E6 (Mindray, Shenzhen, China). Data were analyzed using FlowJo software (TreeStar V.10).

2.11. Statistical Analysis

Results are expressed as the mean \pm SEM or SD. Two-group analyses were performed using an unpaired *t*-test. Three or more groups with one independent variable were analyzed using a one-way ANOVA test. Three or more groups with two independent variables were analyzed using a two-way ANOVA test. The Pearson correlation coefficients and the corresponding *p*-values were calculated using Prism 8 (GraphPad Software, San Diego, CA, USA). Analyses were performed using the Prism 8 (GraphPad Software, San Diego, CA, USA) software. All tests were two-tailed and a *p*-value < 0.05 was considered to indicate statistical significance. All the experiments were repeated a minimum of three times independently to ensure reproducibility.

3. Results

3.1. Study Population, Patient Characteristics and Clinical Responses

In this study, 28 patients with a diagnosis of NSCLC or SCLC who had undergone at least two cycles of PD-L1 inhibitors between 2022 and 2023 were enrolled. Clinical and demographic variables for lung cancer cases are detailed in Table 2. Baseline patient characteristics were as follows: 13 patients had adenocarcinoma (NSCLC) and 15 had SCLC. In total, 3 patients (10.7%) received PD-L1 inhibitors as single agent first-line treatment; 25 patients received PD-L1 inhibitors combined with chemotherapy (89.3%). The median age of the patients was 66.34 years. In total, 7 (25%) patients achieved a total response, 13 (46.4%) remained stable (SD), and 8 (28.6%) showed PD.

Table 2. Patient characteristics.

	1L-IO (n = 3)	ICT (n = 25)
Samples (n)		
BR	2	5
R	1	12
NR	-	8
Age (mean, range)	66.00 (60–75)	66.68 (52–83)
Sex (n, %)		
Female	-	6 (24.00%)
Male	3 (100.00%)	19 (76.00%)
Histology (n, %)		
SCLC	-	15 (60.00%)
NSCLC	3 (100.00%)	10 (40.00%)

BR: best responders; R: responders; NR: non-responders; 1L-IO: patients receiving PD-L1 inhibitors as monotherapy in the first line; ICT: patients receiving chemotherapy plus PD-L1 inhibitors in the second or subsequent lines; 1L: first line; IO: immunotherapy. SCLC: small-cell lung cancer; NSCLC: non-small-cell lung cancer.

3.2. Association of Cytosolic DNA Sensor cGAS/STING Levels in Peripheral Blood with Response to Anti-PD-L1 Blockade

Our group previously reported that the activation of the STING pathway predicts the effectiveness of immunotherapy response in LC [5]. Moreover, CXCL10 and CCL5 are among the two most well-known secreted chemokines activated by the cGAS/STING pathway [14]. Due to limited access to biopsies, particularly from SCLC patients and metastatic NSCLC patients, we aimed to investigate the potential of STING pathway activation through the evaluation of mRNA expression of cGAS-STING and downstream chemokines CXCL10/CCL5 in total PBMCs from LC patients and their correlation to the clinical response to anti-PD-L1 blockade. In Figure 2, the mRNA expression levels of *STING*, *cGAS*, *CXCL10* and *CCL5* in such blood cells were significantly lower ($p < 0.0005$) in the NR cohort as compared to BR. The decrease in mRNA fold change was associated with a poor response to anti-PD-L1 therapy.

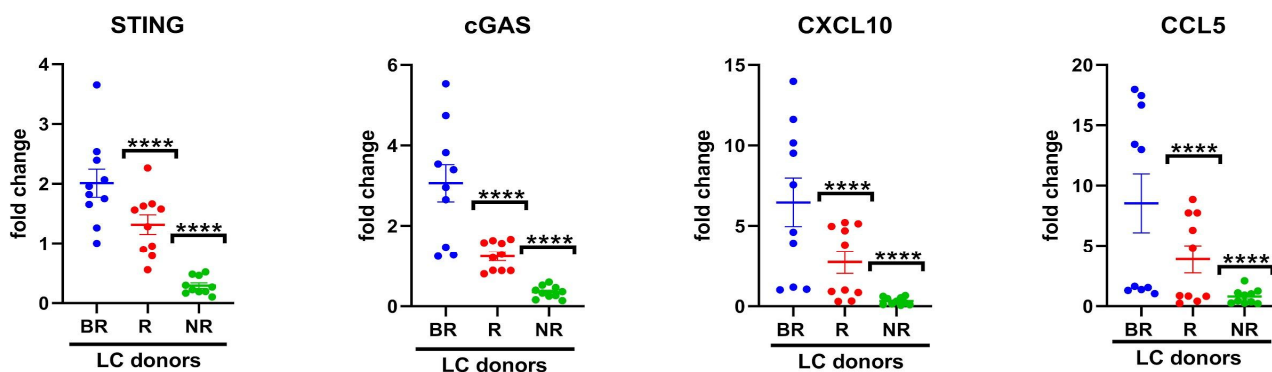


Figure 2. Real-time PCR analysis of in vitro *STING*, *c-GAS*, *CXCL10* and *CCL5* mRNA expression in lung cancer (LC) patient-derived PBMCs. Changes in mRNA levels were normalized to the expression of housekeeping genes (*18S*). Data are expressed as means \pm SEM derived from $n = 2$ technical calculated by the comparative method $2^{-\Delta\Delta C_t}$. One-tailed unpaired Student's *t*-test with CI = 95%, **** $p < 0.0001$.

Furthermore, as shown in Table 3, analysis of expression levels between samples showed positive correlation between the mRNA expression of *STING* and *CXCL10* (Pearson $r = 0.6705$; $p = 0.0339$) in the BR cohort. In R cohort, *STING* mRNA expression positively correlated with *cGAS* (Pearson $r = 0.7053$; $p = 0.0227$), while *cGAS* mRNA expression was also significantly correlated with *CXCL10* (Pearson $r = 0.8643$; $p = 0.0013$) and *CCL5* (Pearson $r = 0.8796$; $p = 0.0008$). Furthermore, in BR and R cohorts, *CXCL10* and *CCL5*

correlated with each other (Pearson $r = 0.8777$; $p = 0.0008$ and Pearson $r = 0.9051$; $p = 0.0003$, respectively). In the NR cohort, *STING* and *cGAS* did not show significant correlations with *CXCL10* or *CCL5* mRNA expression. No significant correlations were found between *CXCL10* and *CCL5* in the NR cohort.

Table 3. Correlation analysis in lung cancer patients (BR, R and NR) between *STING/cGAS* and *CXCL10* and *CCL5* mRNA levels.

BR						
	STING vs. CXCL10	STING vs. CCL5	STING vs. cGAS	cGAS vs. CXCL10	cGAS vs. CCL5	CXCL10 vs. CCL5
r value	0.6705	0.5582	0.3118	0.4053	0.1737	0.8777
95% CI	0.07070 to 0.9142	−0.1102 to 0.8789	−0.3955 to 0.7869	−0.3012 to 0.8245	−0.5119 to 0.7241	0.5545 to 0.9708
p value	0.0339	0.0936	0.3805	0.2452	0.6314	0.0008
R						
	STING vs. CXCL10	STING vs. CCL5	STING vs. cGAS	cGAS vs. CXCL10	cGAS vs. CCL5	CXCL10 vs. CCL5
r value	0.4070	0.4382	0.7053	0.8643	0.8796	0.9051
95% CI	−0.2994 to 0.8252	−0.2643 to 0.8369	0.1362 to 0.9244	0.5149 to 0.9675	0.5602 to 0.9713	0.6405 to 0.9776
p value	0.2431	0.2052	0.0227	0.0013	0.0008	0.0003
NR						
	STING vs. CXCL10	STING vs. CCL5	STING vs. cGAS	cGAS vs. CXCL10	cGAS vs. CCL5	CXCL10 vs. CCL5
r value	−0.1854	0.1827	0.3602	0.08317	0.5195	−0.4806
95% CI	−0.7298 to 0.5030	−0.5050 to 0.7285	−0.3485 to 0.8068	−0.5767 to 0.6773	−0.1637 to 0.8659	−0.8523 to 0.2137
p value	0.6082	0.6134	0.3066	0.8193	0.1238	0.1598

These data suggest that *cGAS-STING* activation is present in PBMCs of patients with clinical response to anti-PD-1/PD-L1 immunotherapy, while it is not detectable in NR patients. *STING* activation is known to be a mediator of PD-1 expression [5], supporting the efficacy of anti-PD-1/PD-L1 agents. Since *cGAS* is not clearly correlated with *STING*, *CXCL10* and *CCL5* mRNA in BR patients, we hypothesize that in this subgroup *STING* may be activated by other immune mediators beyond the canonical *cGAS*-mediated signal. Thus, these data support a further prospective study in a larger population of patients.

3.3. Determination of *STING*-Related Serum Cytokines in Patients with Lung Cancer under Anti-PD1/PD-L1 Therapy

CXCL10/CCL5 serum markers are among the most important published evidence of a potential association with clinical outcome in NSCLC patients receiving PD-L1 inhibitors. The evidence was gathered from 624 original publications identified in PubMed from Schindler H. et al. [15]. Recent evidence showed that DNA damage and accumulation of cytosolic dsDNA leads to activation of the *cGAS*-dependent *STING* pathway in lung adenocarcinoma cells. Specifically, activated T lymphocytes induced DNA damage and activated the *STING* pathway in LC cells [16]. Although various studies on predictive markers in the use of PD-1/PD-L1 inhibitors are in progress, only PD-L1 expression levels in tumor tissues are currently used. Here, we investigated whether baseline serum levels of *CXCL10/CCL5* could represent a good surrogate for the treatment response of patients with advanced NSCLC or SCLC treated with PD-L1 inhibitors. Figure 3 shows a significant reduction of both *CXCL10* and *CCL5* ($p < 0.0001$) in NR serum as compared to BR cohorts. However, analysis shown in Supplementary Table S2 results did not find any significant correlation between serum levels of these proinflammatory chemokines in BR and R patients. These data may be explained by the fact that cytokine/chemokine

baseline levels may be highly variable among patients, thus needing further validation in more extensive sample size studies to find relevant cutoff values. Probably, integration with other features would anyway be necessary for predicting immunotherapy outcome and monitoring the changes over time of these values may be more useful in future studies to better define the cutoff for clinical implications.

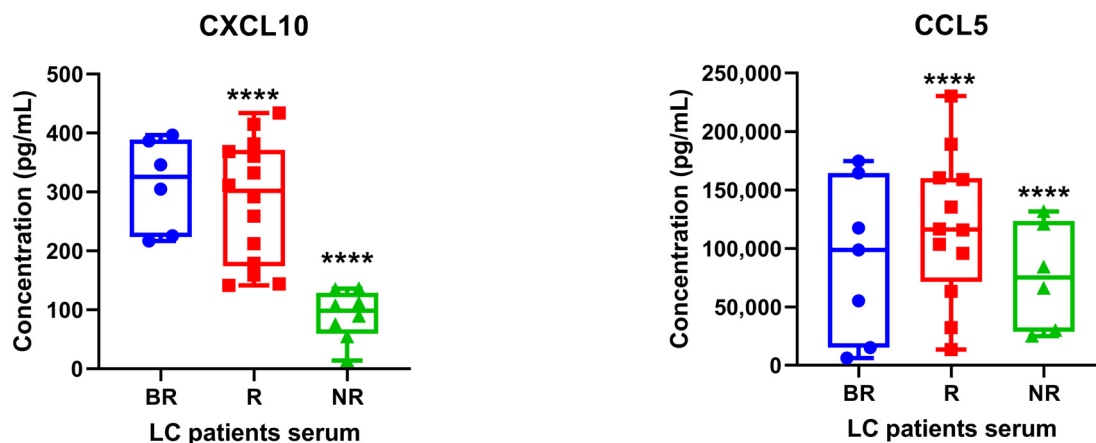


Figure 3. Levels of CXCL10/IP-10 and CCL5 in LC patients' serum were determined using ELISA assay. Each experiment was performed in duplicate. Data represent mean concentrations \pm SD. One-tailed unpaired Student's *t*-test with CI = 95%, **** $p < 0.0001$.

3.4. Germline Variants in DNA Damage Response (DDR) Genes Potentially Implicated in Immune Response

A recent publication showed that about 15% of LC patients harbor a germline pathogenic variant, with a significant enrichment in DDR genes [17]. Pathogenic variants of DDR genes reduce the ability to effectively repair single- and double-strand breaks (SSB and DSB) after DNA damage, thus increasing cancer cell sensitivity to certain therapies. However, the effect of these variants on immune cells is still uncharacterized. Indeed, in a previous publication, we analyzed three long immunotherapy responder patients and found that they presented rare germline variants in DDR genes [8]. Independently from their putative role in cancer induction/promotion, as immune cells are the main effectors of immunotherapy, we aimed at investigating the possible presence of these variants in a larger patient cohort. Moreover, based on mRNA correlation results in NR patients, we looked for further targets in the NR cohort by performing germline analysis. Therefore, all patients underwent germline genetic testing focusing on a panel of DDR genes according to our previous publication [8]. Interestingly, we identified heterozygous germline LoF variants in DDR genes (Table 4). In particular, we found germline *POLE*, *POLD1*, *RAD51* *paralog B* (*RAD51B*), checkpoint kinase 1 (*CHEK1*) and *ATM* pathogenic variants in BR and R SCLC patients, whereas NSCLC BR/R patients harbored germline pathogenic variants in *BARD1* and *ATM* (Figure 4) [8,18–21]. Importantly, no germline variants in the DDR genes panel were found in the NR cohort. This trend, if later validated in a larger cohort of patients, may suggest that deleterious DDR variants in the PBMCs of LC patients might have an impact on their clinical response to immunotherapy. In contrast, LC patients with no deleterious DDR variants may be less responsive to treatments.

Table 4. Mutated DDR gene names and number of pathogenic variants in corresponding patient’s ID of SCLC and NSCLC are shown. We found germline heterozygous variants in all genes reported in the table. Variant read frequency is expressed as absolute value.

Patient ID	Genes	HGVSP	Consequence	Sift Prediction	PolyPhen Prediction	Variant Read Frequency	ClinVar
NSCLC_1	BARD1	p.(Arg406Ter)	stop_gained	-	-	0.48421052	VCV000229677.13: pathogenic
NSCLC_2	ATM	p.(Ser333Phe)	missense_variant	deleterious	probably damaging	0.47340426	VCV000127471.16: uncertain significance
NSCLC_3	BARD1	p.(Asp673Tyr)	missense_variant	deleterious	probably damaging	0.55279505	VCV000482778.3: uncertain significance
SCLC_1	CHEK2	p.(Asn105IlefsTer11)	frameshift_variant	-	-	0.19469027	-
	POLE	p.(Lys425Arg)	missense_variant	deleterious	probably damaging	0.46486485	VCV000224587.7: uncertain significance
	RAD51B	p.(Lys243Arg)	missense_variant	deleterious	probably damaging	0.16216215	-
SCLC_2	APOBEC1	p.(Glu41Gln)	missense_variant	deleterious	-	0.53571427	-
	FANCC	p.(Asp195Val)	missense_variant	deleterious	probably damaging	0.556701	VCV000134305.15: uncertain significance
SCLC_3	APOBEC4	p.(Arg183Trp)	missense_variant	tolerated	-	0.43418014	-
	ATM	p.(Ser49Cys)	missense_variant	deleterious	possibly damaging	0.5242967	VCV000003048.16: uncertain significance
	APOBEC1	p.(Pro108Ser)	missense_variant	deleterious	-	0.50517243	-
SCLC_4	POLD1	p.(Gln53Ter)	stop_gained	-	-	0.44516128	-
SCLC_5	-	-	-	-	-	-	-
SCLC_6	-	-	-	-	-	-	-
SCLC_7	-	-	-	-	-	-	-

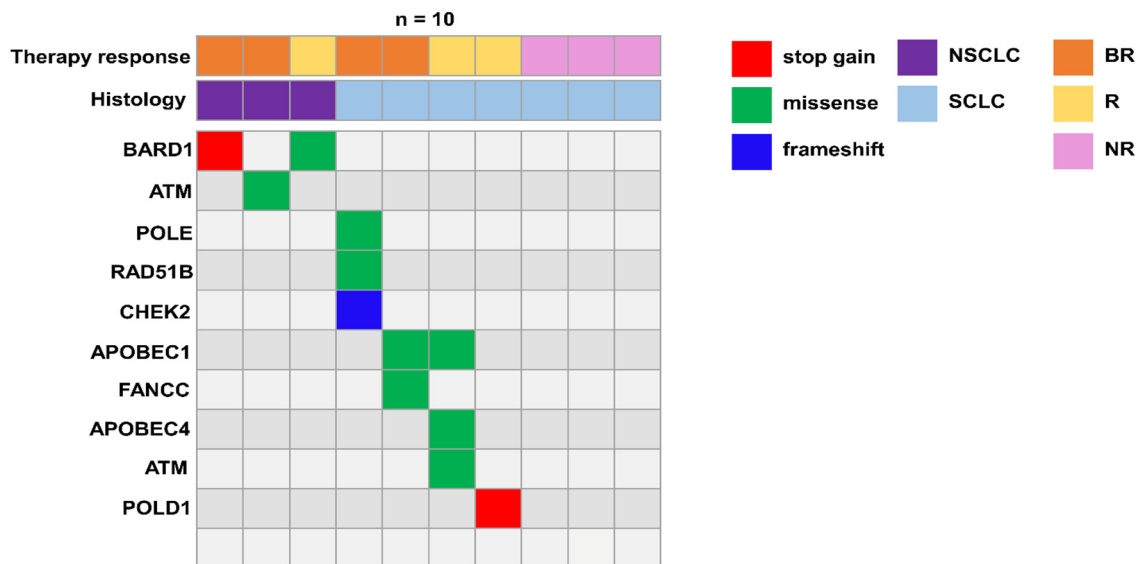


Figure 4. Gene name, variant types and number of variants of pathogenic DDR germline variants found in LC patients. Type and the therapy response of the corresponding LC groups are shown.

3.5. Effect of DNA-Dependent Protein Kinase (DNA-PK) Inhibitor on Cytosolic DNA Sensor cGAS/STING in Peripheral Blood of LC with Different Response to Anti-PD-L1 Blockade

As we did not find any functional alterations of DDR proteins in patients less responsive to immunotherapy, we hypothesized that their more functional state compared to BR might mediate immunotherapy resistance. Therefore, we tested a DDR inhibitor, DNA-PK-I, on PBMCs from LC patients according to the clinical responses to anti-PD1/PD-L1 therapy. As shown in Figure 5, NR patients respond to DNA-PK-I with a significant

increase in the cGAS/STING pathway, suggesting that inhibition of this pathway is an important requirement for the activation of mediated immunity in PBMCs. The strong increase in *cGAS/STING* mRNA levels in response to DNA-PK inhibition in NR patients may be explained by the effect on perturbation by the drug on DDR machinery. On the other hand, because the DDR machinery is genetically altered in the BR and R cohorts, this may represent the intrinsic mechanism that also causes DNA damage-dependent cGAS/STING pathway activation in immune cells.

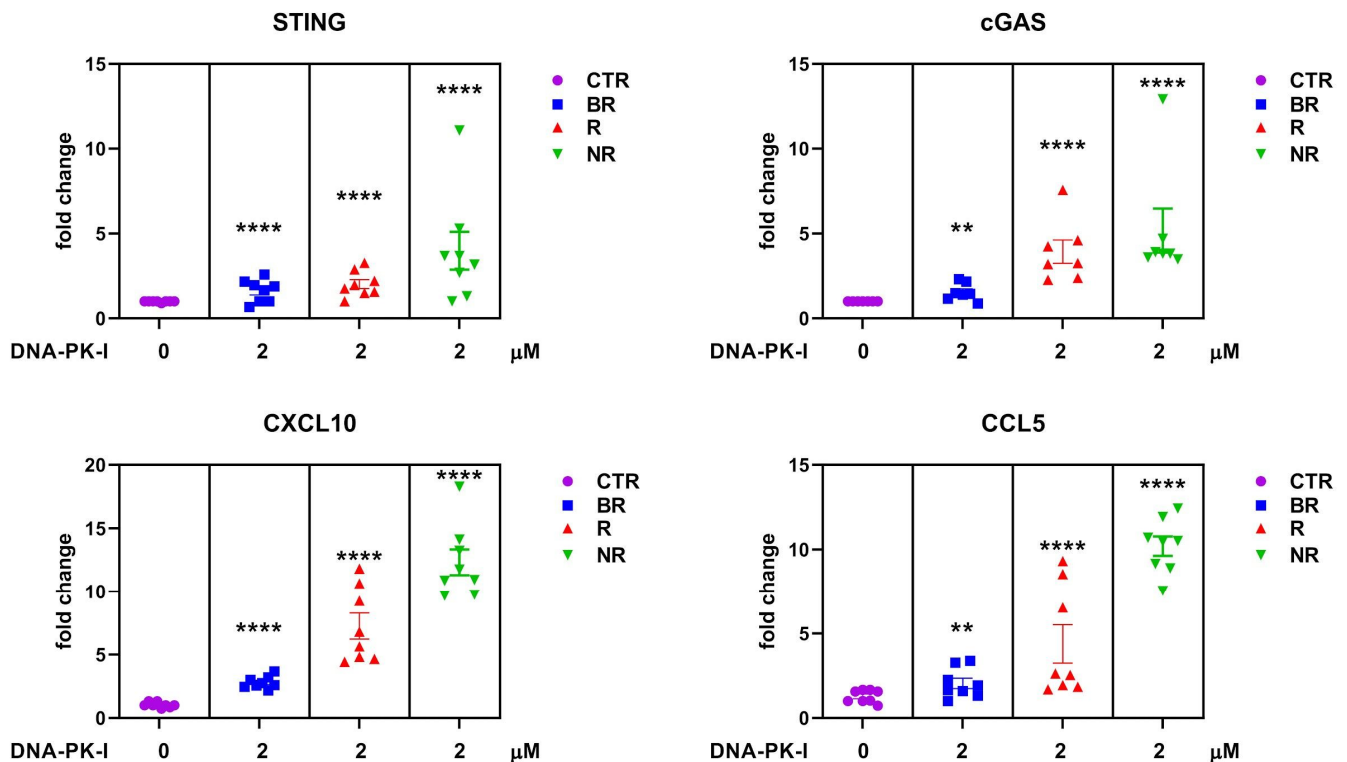


Figure 5. The mRNA expression levels of *STING*, *cGAS*, *CXCL10* and *CCL5* were studied by RT-qPCR in LC patient-derived PBMCs cultured in complete media supplemented with 10% HS for 24 h and then treated with DNA-PK-I 2 μM for 72 h; *18S* was used as the reference gene. Results are expressed as means ± SEM derived from $n = 2$ technical calculated by the comparative method $2^{-\Delta\Delta C_t}$. One-tailed unpaired Student's *t*-test with CI = 95%, **** $p < 0.0001$, ** $p < 0.05$.

Taken together, these results suggest that PBMCs from LC patients may be a tool to study the activation of immune pathways with novel drugs such as DDR inhibitors that are under clinical investigation for LC; also, these results may be of interest if correlated with the presence of germline DDR gene alterations as potential novel biomarkers.

3.6. Antitumoral Activity and Innate Immune Cells Effect of DNA-PK Inhibitor

Here, we aimed to evaluate the functional effect of cisplatin, the standard of care for LC patients in combination with immunotherapy, on LC patient-derived PBMCs. Specifically, we tested the applicability of PBMCs as an *in vitro* tool to study and reproduce the effect of cisplatin on immune cells in the tumor microenvironment. Additionally, we evaluated the effect of DNA-PK-I as a potential candidate drug to activate PBMCs based on a similar effect on DNA damage and DDR machinery perturbation in a chemotherapy-like way. We propose a 3D co-culture model of different types of lung cancer cell lines (H460, H661 and A549) and LC patient-derived PBMCs. As showed in Figure 6, untreated PBMCs from LC patients were not able to access the compact 3D tumor structure. Interestingly, cisplatin-treated immune cells infiltrated the spheroids at day 5 and the spheroid's 3D structure was destroyed (Figure 6). We also used DNA-PK-I pre-treated PBMCs as controls

for DNA damage induction since it has been widely demonstrated that DNA-damaging therapies induce a DNA sensor STING-dependent antitumor immune response [5,22]. Quantitative analysis showed that both cisplatin and DNA-PK-I were able to significantly increase the red/blue intensity ratio in H460 (Figure 6A), H661 (Figure 6B) and A549 (Figure 6C), indicating an increased infiltration ability towards the 3D tumor spheroids. Taken together, these results demonstrated that 3D co-culture models of tumor spheroids and PBMCs represent a valid surrogate of mouse models for functional in vitro prediction of therapy-induced immune system activation and strengthen the rationale for more tailored mechanistic studies in animal models. Moreover, the results obtained with DNA-PK-I potentially open up new treatment options for NR patients to be tested in a clinical setting.

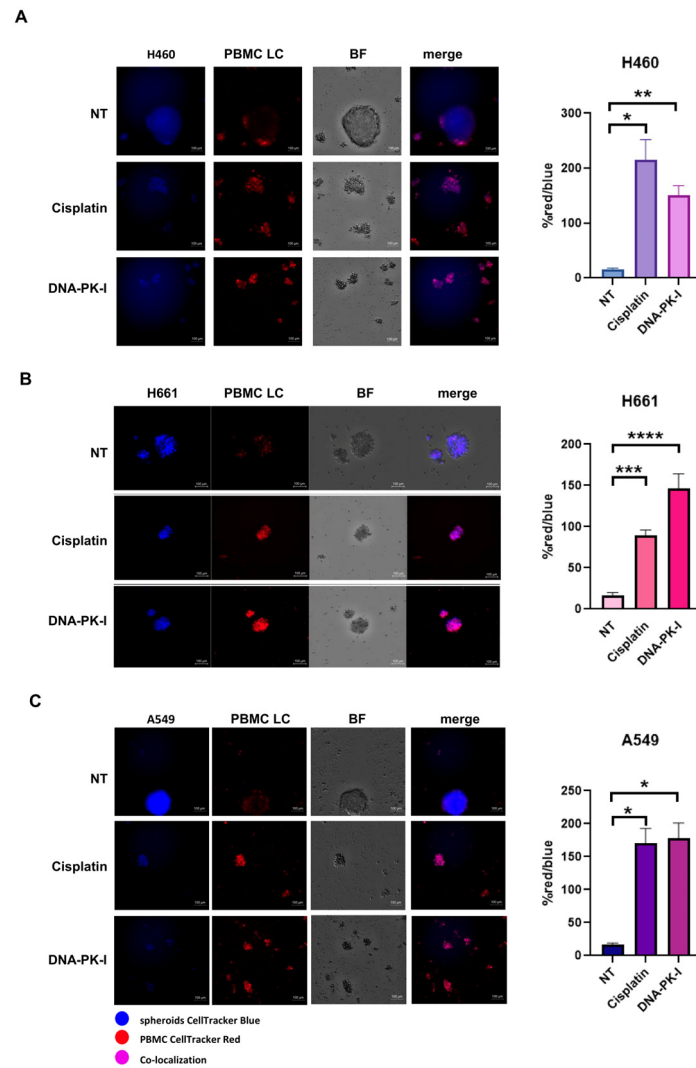


Figure 6. (A–C) Representative immunofluorescence images showing the infiltration ability of immune cells in 3D tumor spheroids of H460 (A), H661 (B) and A549 (C) cells and evaluation of the red/blue intensity ratio as a quantitative indication of the co-localization rate of LC cells and PBMC. Statistical significance: **** $p < 0.0001$, *** $p < 0.001$, ** $p < 0.01$, * $p < 0.05$. Three-dimensional tumor spheroids were blue stained, and the LC patient-derived PBMCs were red stained. The PBMCs were pre-treated with DNA-PK-I (2 μM) or cisplatin (0.5 μM) for 72 h and then added to 3D spheroids to start the co-culture. The co-localization of LC cells and PBMCs is reported under the merge column. Scale bar 100 μm .

3.7. Subpopulation Analysis of STING Expression in LC Patient-Derived PBMCs

Since PBMCs are extremely heterogeneous, to further analyze which subset was more implicated in cGAS/STING activation, we examined PBMCs derived from LC patients from the BR, R and NR cohorts by flow cytometry and determined which gated subpopulation displayed a higher STING expression. CD8+ T cell subsets were significantly enriched in the BR and R cohorts, as shown in Figure 7A. In addition, the BR cohorts also showed a higher percentage of NK cells compared to the R and NR cohorts. Among the PBMC gated subsets derived from LC patients, the percentage of STING-positive cells was significantly higher in CD8+ T cells. These results indicate that cytotoxic T lymphocytes (CTLs) and natural killer (NK) cells are the predominant subset among lymphocytes in BR PBMCs derived from LC patients. In addition, CTLs are the major contributors to STING expression in PBMCs derived from LC patients. To further confirm our findings, we assessed the cytotoxic activity of innate immune cells by determination of cytokine and cytotoxic granule protein levels. In particular, we focused on the secretion of granzyme A, granzyme B, perforin and granulysin, which are mainly secreted by CTLs and NK cells. In addition, they are highly associated with the innate immune response to various intracellular pathogens as well as tumors [8,23,24]. Therefore, we quantified these mediators in culture supernatants of LC patient-derived PBMCs by multiplex analysis. As shown in Figure 7B, we found that the BR cohort highly secreted granzyme A, granzyme B, perforin and granulysin as compared to the NR cohort. Taken together, these results suggest that cGAS/STING activation in CTLs, which are most known for releasing proteins contained within the cytolytic granules, positively influences the antitumor cytotoxic activity of innate immune cells.

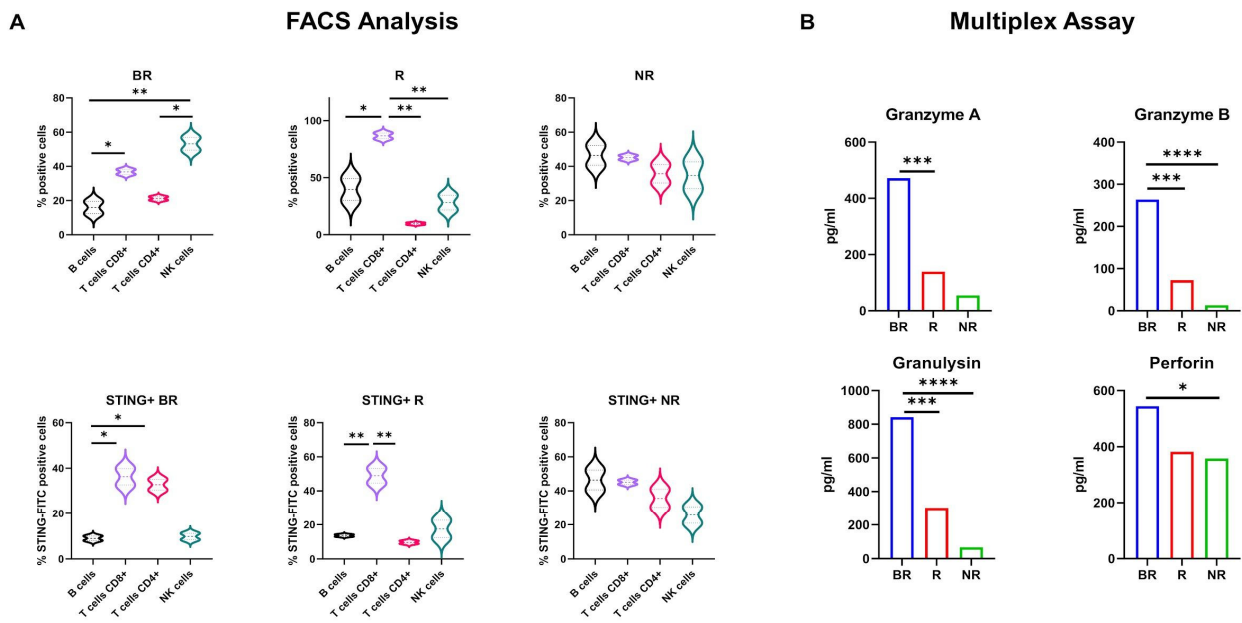


Figure 7. (A) FACS analysis of LC patient-derived PBMC subset (upper panel) and % of STING-positive cells (lower panel). Statistical significance: ** $p < 0.001$, * $p < 0.05$. (B) Luminex cytokine assay of granzyme A, granzyme B, granulysin and perforin in LC patient-derived PBMC culture supernatant. **** $p < 0.0001$, *** $p < 0.001$, * $p < 0.05$.

4. Discussion

Despite a large number of candidate biomarkers under clinical investigation to select patients for immunotherapy, only a limited number of molecular assays based on PD-L1 expression are currently approved by the FDA. In particular, these noninvasive tests have been clinically validated to identify patients more likely to benefit from single-agent anti-PD-1/PD-L1 therapy. However, due to the complex interplay between immune reaction and tumor biology, a more accurate analysis will be relevant to predict patient response

to immune-targeted therapy. Indeed, accurate prediction of clinical benefit may require combination of multiple tumor and immunological response markers, such as protein expression, genomics and transcriptomics. For example, in syngeneic mouse models of cancer, an antitumor immunity effect has been observed following intratumoral administration of a STING agonist [25]. Furthermore, the effects of radiotherapy [26], checkpoint inhibitors [5] and, recently, PARP inhibitors [27], are highly dependent on the presence of STING, and anti-cancer effects are enhanced when combined with STING agonists. In a cancer setting, it is obviously necessary to study immune status and activation within the cancer site, but the peripheral immune system can also provide important information, particularly on intrinsic function and immune response capacity. Considering the low availability of tissue material from LC patients, in this work we provided evidence of using PBMCs as a new tool for biomarker study. Further investigations will be carried out to evaluate the applicability of these results to transform SCLC that is derived from NSCLC. Even if we recognize the potential limit of inter-patient variability, with this pivotal study we had a coherent result in terms of immune system activation and clinical response to anti-PD-L1 in PBMCs by testing STING-related markers. Moreover, PBMCs allowed us also to perform functional studies that may be useful to predict immune system activation *ex vivo*, as exemplified by the changes in the gene expression profile or immune cell infiltration during treatment with DNA-PK-I or chemotherapy. As immunotherapy lacks valid and predictive peripheral biomarkers and lymphocytes play a key role in tumor killing in immunotherapy, another aim of the present study was to understand whether germline variants in DDR genes may suggest a new target for poor responders to anti-PD-L1 drugs. To date, no ATLAS of PBMC germline variants predicting immunotherapy response exists in the literature. We selected genes of interest using the DDR panel and found that there are variants in responding patients that may be of greater clinical importance in predicting response to immunotherapy. Although this was a small cohort, in view of the scientific evidence reported, we hypothesize that this genetic predisposition could interplay with additional acquired mutations within the tumor that may contribute to modulate response to immunotherapy. We can conclude that PBMCs may be a good tool for study of biomarkers of response to immunotherapy based on *cGAS/STING* mRNA levels in LC patients. On the other hand, the analysis of CXCL10 and CCL5 expression in serum together with the analysis of the germline DDR panel need future studies. Serum analysis should be extended to a larger population, especially to understand this large variability at baseline in patients that may be affected by multiple inflammation triggers.

5. Conclusions

In conclusion, we used for the first time PBMCs from LC patients during immunotherapy as a tool to investigate features of immune responsiveness. We found that *cGAS/STING* activation in PBMCs, mainly in cytotoxic lymphoid cells, together with rare germline variants in the DDR gene panel, may be a useful tool to predict response to immunotherapy in LC patients but requires further confirmation in a larger number of patients. Moreover, we found that NR LC patients with absence of rare germline variants in DDR genes are potential candidates for a rationale of using DDRi in clinical practice.

Supplementary Materials: The following supporting information can be downloaded at: <https://www.mdpi.com/article/10.3390/biomedicines12040809/s1>, Table S1: Cytokine assay characteristics; Table S2: Correlation analysis of CXCL10 and CCL5 ELISA.

Author Contributions: Conceptualization: F.M. and C.M.D.C. methodology: C.D.R., F.I., C.T., G.E., L.A., A.A., F.P., G.d.G. and D.C.; validation: C.D.R., F.I., C.T., L.A., F.P., V.T., A.A., G.F., A.d.L. and E.M.; formal analysis: C.D.R., F.I., V.D.R., F.P., V.T., F.C. (Flora Cimmino), G.M., F.M. and C.M.D.C.; writing—original draft preparation: C.D.R., F.I., V.D.R., F.M. and C.M.D.C.; writing—review and editing: C.D.R., F.I., V.D.R., F.P., T.T., S.N., F.C. (Fortunato Ciardiello), F.S., G.E. and C.M.D.C.; supervision: F.C., F.M. and C.M.D.C.; funding acquisition: C.M.D.C. All authors have read and agreed to the published version of the manuscript.

Funding: This work was supported by Fondazione AIRC (MFAG Project Number: 26237 to C.M.D.C.; MFAG Project number: 26002 to G.E.; and SIS Project number: 28705 to F.S.).

Institutional Review Board Statement: The study was conducted in accordance with the Declaration of Helsinki, and approved by the Ethics Committee of the University of Campania “Luigi Vanvitelli”, Naples (n. 280 on 16 May 2020).

Informed Consent Statement: Informed consent was obtained from all subjects involved in the study.

Data Availability Statement: The majority of data related to presented results are included in the materials and methods section of the paper. NGS raw data were generated at facility center Ames (Casalnuovo, Napoli) and are available from the corresponding authors C.M.D.C. or V.D.R. on request.

Conflicts of Interest: Dr. Morgillo F.: receipt of honoraria or consultation fees for speaker, consultancy, or advisory roles: Roche, Servier, Incyte, ESMO and MSD. Dr. Papaccio F.: private research funding from Merck, travel support from Diotech Pharmacogenetics and recipient of an ESMO Research Fellowship sponsored by Amgen from 2018 to 2020. Dr. Ciardiello D.: travel support from Sanofi, BMS and Merck KgA. Dr. Martinelli E.: receipt of honoraria or consultation fees for speaker, consultancy or advisory roles: Amgen, Bayer, Eisai, Merck Serono, Pierre Fabre, Roche, Servier, Incyte, ESMO, MSD; travel grant: AstraZeneca, Pierre Fabre. Dr. Troiani T.: receipt of honoraria or consultation fees for speaker, consultancy, or advisory roles: Merck, Amgen, Pierre Fabre, Servier, MSD, Bayer and Novartis. Dr. Napolitano S.: received travel grants from Amgen, Merck KGaA, Bristol Myers Squibb and Novartis outside the submitted work. Dr. Martini G.: reported receiving honoraria from Servier and Incyte outside the submitted work. Dr. Ciardiello F.: receipt of honoraria or consultation fees for speaker, consultancy, or advisory roles: Amgen, Merck KGaA, MSD, Pierre Fabre, Pfizer, Roche Servier; institutional financial interests, financial support for clinical trials or contracted research; Amgen, Merck KGaA, MSD, Pierre Fabre, Pfizer, Roche, Servier. Dr. Della Corte C.M.: reported receiving personal fees from Roche, MSD and AstraZeneca, and travel grants from Amgen outside the submitted work. The remaining authors have no conflicts of interest to declare.

References

1. Lahiri, A.; Maji, A.; Potdar, P.D.; Singh, N.; Parikh, P.; Bisht, B.; Mukherjee, A.; Paul, M.K. Lung cancer immunotherapy: Progress, pitfalls, and promises. *Mol. Cancer* **2023**, *22*, 40. [[CrossRef](#)] [[PubMed](#)]
2. Horvath, L.; Thienpont, B.; Zhao, L.; Wolf, D.; Pircher, A. Overcoming immunotherapy resistance in non-small cell lung cancer (NSCLC)—Novel approaches and future outlook. *Mol. Cancer* **2020**, *19*, 141. [[CrossRef](#)] [[PubMed](#)]
3. Lv, M.; Chen, M.; Zhang, R.; Zhang, W.; Wang, C.; Zhang, Y.; Wei, X.; Guan, Y.; Liu, J.; Feng, K.; et al. Manganese is critical for antitumor immune responses via cGAS-STING and improves the efficacy of clinical immunotherapy. *Cell Res.* **2020**, *30*, 966–979. [[CrossRef](#)] [[PubMed](#)]
4. Fan, T.W.; Higashi, R.M.; Song, H.; Daneshmandi, S.; Mahan, A.L.; Purdom, M.S.; Bocklage, T.J.; Pittman, T.A.; He, D.; Wang, C.; et al. Innate immune activation by checkpoint inhibition in human patient-derived lung cancer tissues. *eLife* **2021**, *10*, e69578. [[CrossRef](#)] [[PubMed](#)]
5. Della Corte, C.M.; Sen, T.; Gay, C.M.; Ramkumar, K.; Diao, L.; Cardnell, R.J.; Rodriguez, B.L.; Stewart, C.A.; Papadimitrakopoulou, V.A.; Gibson, L.; et al. STING Pathway Expression Identifies NSCLC with an Immune-Responsive Phenotype. *J. Thorac. Oncol.* **2020**, *15*, 777–791. [[CrossRef](#)] [[PubMed](#)]
6. Lee, Y.J.; Park, Y.S.; Lee, H.W.; Park, T.Y.; Lee, J.K.; Heo, E.Y. Peripheral lymphocyte count as a surrogate marker of immune checkpoint inhibitor therapy outcomes in patients with non-small-cell lung cancer. *Sci. Rep.* **2022**, *12*, 626. [[CrossRef](#)] [[PubMed](#)]
7. Kim, K.H.; Cho, J.; Ku, B.M.; Koh, J.; Sun, J.M.; Lee, S.H.; Ahn, J.S.; Cheon, J.; Min, Y.J.; Park, S.H.; et al. The First-week Proliferative Response of Peripheral Blood PD-1. *Clin. Cancer Res.* **2019**, *25*, 2144–2154. [[CrossRef](#)] [[PubMed](#)]
8. Della Corte, C.M.; Fasano, M.; Ciaramella, V.; Cimmino, F.; Cardnell, R.; Gay, C.M.; Ramkumar, K.; Diao, L.; Di Liello, R.; Viscardi, G.; et al. Anti-tumor activity of cetuximab plus avelumab in non-small cell lung cancer patients involves innate immunity activation: Findings from the CAVE-Lung trial. *J. Exp. Clin. Cancer Res.* **2022**, *41*, 109. [[CrossRef](#)] [[PubMed](#)]
9. Reck, M.; Rodríguez-Abreu, D.; Robinson, A.G.; Hui, R.; Csósz, T.; Fülöp, A.; Gottfried, M.; Peled, N.; Tafreshi, A.; Cuffe, S.; et al. Pembrolizumab versus Chemotherapy for PD-L1-Positive Non-Small-Cell Lung Cancer. *N. Engl. J. Med.* **2016**, *375*, 1823–1833. [[CrossRef](#)]
10. Novello, S.; Kowalski, D.M.; Luft, A.; Gümüş, M.; Vicente, D.; Mazières, J.; Rodríguez-Cid, J.; Tafreshi, A.; Cheng, Y.; Lee, K.H.; et al. Pembrolizumab Plus Chemotherapy in Squamous Non-Small-Cell Lung Cancer: 5-Year Update of the Phase III KEYNOTE-407 Study. *J. Clin. Oncol.* **2023**, *41*, 1999–2006. [[CrossRef](#)]
11. Horn, L.; Mansfield, A.S.; Szczesna, A.; Havel, L.; Krzakowski, M.; Hochmair, M.J.; Huemer, F.; Losonczy, G.; Johnson, M.L.; Nishio, M.; et al. First-Line Atezolizumab plus Chemotherapy in Extensive-Stage Small-Cell Lung Cancer. *N. Engl. J. Med.* **2018**, *379*, 2220–2229. [[CrossRef](#)] [[PubMed](#)]

12. Della Corte, C.M.; Barra, G.; Ciaramella, V.; Di Liello, R.; Vicidomini, G.; Zappavigna, S.; Luce, A.; Abate, M.; Fiorelli, A.; Caraglia, M.; et al. Antitumor activity of dual blockade of PD-L1 and MEK in NSCLC patients derived three-dimensional spheroid cultures. *J. Exp. Clin. Cancer Res.* **2019**, *38*, 253. [[CrossRef](#)] [[PubMed](#)]
13. Fasano, M.; Della Corte, C.M.; Di Liello, R.; Barra, G.; Sparano, F.; Viscardi, G.; Iacovino, M.L.; Paragliola, F.; Famiglietti, V.; Ciaramella, V.; et al. Induction of natural killer antibody-dependent cell cytotoxicity and of clinical activity of cetuximab plus avelumab in non-small cell lung cancer. *ESMO Open* **2020**, *5*, e000753. [[CrossRef](#)] [[PubMed](#)]
14. Taniguchi, H.; Caeser, R.; Chavan, S.S.; Zhan, Y.A.; Chow, A.; Manoj, P.; Uddin, F.; Kitai, H.; Qu, R.; Hayatt, O.; et al. WEE1 inhibition enhances the antitumor immune response to PD-L1 blockade by the concomitant activation of STING and STAT1 pathways in SCLC. *Cell Rep.* **2022**, *39*, 110814. [[CrossRef](#)]
15. Schindler, H.; Lusky, F.; Daniello, L.; Elshiaty, M.; Gaissmaier, L.; Benesova, K.; Souto-Carneiro, M.; Angeles, A.K.; Janke, F.; Eichhorn, F.; et al. Serum cytokines predict efficacy and toxicity, but are not useful for disease monitoring in lung cancer treated with PD-(L)1 inhibitors. *Front. Oncol.* **2022**, *12*, 1010660. [[CrossRef](#)] [[PubMed](#)]
16. Xiong, H.; Xi, Y.; Yuan, Z.; Wang, B.; Hu, S.; Fang, C.; Cai, Y.; Fu, X.; Li, L. IFN- γ activates the tumor cell-intrinsic STING pathway through the induction of DNA damage and cytosolic dsDNA formation. *Oncimmunology* **2022**, *11*, 2044103. [[CrossRef](#)] [[PubMed](#)]
17. Sorscher, S.; LoPiccolo, J.; Heald, B.; Chen, E.; Bristow, S.L.; Michalski, S.T.; Nielsen, S.M.; Lacoste, A.; Keyder, E.; Lee, H.; et al. Rate of Pathogenic Germline Variants in Patients with Lung Cancer. *JCO Precis. Oncol.* **2023**, *7*, e2300190. [[CrossRef](#)] [[PubMed](#)]
18. Garmezay, B.; Gheeya, J.; Lin, H.Y.; Huang, Y.; Kim, T.; Jiang, X.; Thein, K.Z.; Pilié, P.G.; Zeineddine, F.; Wang, W.; et al. Clinical and Molecular Characterization of. *JCO Precis. Oncol.* **2022**, *6*, e2100267. [[CrossRef](#)] [[PubMed](#)]
19. Pecori, R.; Di Giorgio, S.; Paulo Lorenzo, J.; Nina Papavasiliou, F. Functions and consequences of AID/APOBEC-mediated DNA and RNA deamination. *Nat. Rev. Genet.* **2022**, *23*, 505–518. [[CrossRef](#)]
20. Guerreiro, I.M.; Barros-Silva, D.; Lopes, P.; Cantante, M.; Cunha, A.L.; Lobo, J.; Antunes, L.; Rodrigues, A.; Soares, M.; Henrique, R.; et al. Levels as a Potential Predictive Biomarker for PD-1 Blockade Response in Non-Small Cell Lung Cancer. *J. Clin. Med.* **2020**, *9*, 1000. [[CrossRef](#)]
21. Yi, R.; Lin, A.; Cao, M.; Xu, A.; Luo, P.; Zhang, J. ATM Mutations Benefit Bladder Cancer Patients Treated with Immune Checkpoint Inhibitors by Acting on the Tumor Immune Microenvironment. *Front. Genet.* **2020**, *11*, 933. [[CrossRef](#)] [[PubMed](#)]
22. Concannon, K.; Morris, B.B.; Gay, C.M.; Byers, L.A. Combining targeted DNA repair inhibition and immune-oncology approaches for enhanced tumor control. *Mol. Cell* **2023**, *83*, 660–680. [[CrossRef](#)] [[PubMed](#)]
23. Pardo, J.; Aguilo, J.I.; Anel, A.; Martin, P.; Joeckel, L.; Borner, C.; Wallich, R.; Müllbacher, A.; Froelich, C.J.; Simon, M.M. The biology of cytotoxic cell granule exocytosis pathway: Granzymes have evolved to induce cell death and inflammation. *Microbes Infect.* **2009**, *11*, 452–459. [[CrossRef](#)]
24. Boivin, W.A.; Cooper, D.M.; Hiebert, P.R.; Granville, D.J. Intracellular versus extracellular granzyme B in immunity and disease: Challenging the dogma. *Lab. Invest.* **2009**, *89*, 1195–1220. [[CrossRef](#)] [[PubMed](#)]
25. Wu, Y.T.; Fang, Y.; Wei, Q.; Shi, H.; Tan, H.; Deng, Y.; Zeng, Z.; Qiu, J.; Chen, C.; Sun, L.; et al. Tumor-targeted delivery of a STING agonist improves cancer immunotherapy. *Proc. Natl. Acad. Sci. USA* **2022**, *119*, e2214278119. [[CrossRef](#)] [[PubMed](#)]
26. Huang, K.C.; Chiang, S.F.; Chang, H.Y.; Chen, W.T.; Yang, P.C.; Chen, T.W.; Liang, J.A.; Shiau, A.C.; Ke, T.W.; Clifford Chao, K.S. Engineered sTRAIL-armed MSCs overcome STING deficiency to enhance the therapeutic efficacy of radiotherapy for immune checkpoint blockade. *Cell Death Dis.* **2022**, *13*, 610. [[CrossRef](#)]
27. Byers, L.A.; Wang, J.; Nilsson, M.B.; Fujimoto, J.; Saintigny, P.; Yordy, J.; Giri, U.; Peyton, M.; Fan, Y.H.; Diao, L.; et al. Proteomic profiling identifies dysregulated pathways in small cell lung cancer and novel therapeutic targets including PARP1. *Cancer Discov.* **2012**, *2*, 798–811. [[CrossRef](#)]

Disclaimer/Publisher’s Note: The statements, opinions and data contained in all publications are solely those of the individual author(s) and contributor(s) and not of MDPI and/or the editor(s). MDPI and/or the editor(s) disclaim responsibility for any injury to people or property resulting from any ideas, methods, instructions or products referred to in the content.